



Provided for non-commercial research and education use.
Not for reproduction, distribution or commercial use.


Volume 40, issue 6 April 2008 ISSN 1386-9477



PHYSICA
Recognized by the European Physical Society




**LOW-DIMENSIONAL SYSTEMS
& NANOSTRUCTURES**



Proceedings of the 13th International
Conference on Modulated
Semiconductor Structures
(MSS-13)

held in Genova, Italy
15–20 July 2007

Guest Editors:
G. Goldoni
L. Sorba

Available online at
 **ScienceDirect**
www.sciencedirect.com

<http://www.elsevier.com/locate/physa>

This article appeared in a journal published by Elsevier. The attached copy is furnished to the author for internal non-commercial research and education use, including for instruction at the authors institution and sharing with colleagues.

Other uses, including reproduction and distribution, or selling or licensing copies, or posting to personal, institutional or third party websites are prohibited.

In most cases authors are permitted to post their version of the article (e.g. in Word or Tex form) to their personal website or institutional repository. Authors requiring further information regarding Elsevier's archiving and manuscript policies are encouraged to visit:

<http://www.elsevier.com/copyright>



Nanoscale heat transfer in quantum cascade lasers

Gaetano Scamarcio^{a,*}, Miriam S. Vitiello^a, Vincenzo Spagnolo^b, Sushil Kumar^c,
Benjamin Williams^c, Qing Hu^c

^aCNR-INFM Regional Laboratory LIT³ and Dipartimento Interateneo di Fisica “M. Merlin”, Università degli Studi di Bari,
Via Amendola 173, 70126 Bari, Italy

^bCNR-INFM Regional Laboratory LIT³ and Dipartimento Interateneo di Fisica “M. Merlin”, Politecnico di Bari, Via Amendola 173, 70126 Bari, Italy

^cDepartment of Electrical Engineering and Computer Science and Research Laboratory of Electronics, Massachusetts Institute of Technology,
Cambridge, MA 02139, USA

Available online 7 October 2007

Abstract

We have measured the local lattice temperature distribution and modeled the heat transport in all classes of quantum cascade lasers operating both in the mid-infrared and terahertz ranges. All relevant active regions based on GaAs/AlGaAs, GaInAs/AlGaAsSb, GaInAs/AlInAs/InP material systems have been investigated. A common feature of such complex multiple heterostructures is the strong anisotropy of thermal conductivity, its cross-plane component being much smaller than the in-plane one. Bulk contributions to this phenomenon are negligible, whereas a dominant role is played by the presence of abrupt sub-nanometer sized interfaces. The presence of a high density of interfaces causes phonon interference effects, which inherently limit the heat extraction. The values of the thermal boundary resistance have been extracted from our experimental data and compared among several devices. The possibility of generating stimulated emission of phonons in terahertz quantum cascade lasers will be also discussed.

© 2007 Elsevier B.V. All rights reserved.

PACS: 61.46.w; 61.82.FK; 68.35.Ct

Keywords: Nanoscale materials; Semiconductors; Interface structure and roughness

1. Introduction

Quantum cascade lasers (QCLs) are unipolar semiconductor devices based on the engineering of electronic wavefunctions at the nanoscale level in multiple quantum well structures. Heat extraction from QCLs is difficult because of three main reasons: (i) the high electrical power (P); (ii) the large device thermal resistance due to the low heat conductivity of QCL active regions; and (iii) the poor thermal coupling between the active region and the heat sink related with the waveguide and mounting configurations.

The device thermal conductivity is anisotropic and both the in-plane (k_{\parallel}) and cross-plane (k_{\perp}) components have smaller values than bulk constituent materials due to

nanoscale phenomena [1–3]. In semiconductor multi-layered heterostructures like QCLs, the layer widths are comparable or smaller than the phonon mean free path. This causes the increase of the rate of phonon scattering by interfaces, inhibits phonon transport and reduces the heat dissipation rate [1,2]. The reduction of the in-plane component can be explained by partly diffusive scattering of phonons at the interfaces [1]. Several causes can affect the much higher reduction of k_{\perp} : (i) the reduction of the group velocities of phonons, especially high-energy acoustic phonons; (ii) the multiple phonon reflection induced by the mismatch in the phonon dispersion at the interface; and (iii) the scattering by interface roughness or alloy disorder [1,2,4].

Knowledge of the active region thermal conductivity and of its temperature dependence is mandatory for modeling heat flows and local temperature distributions in QCLs. The use of an isotropic model for the active region thermal

*Corresponding author. Tel./fax: +80 5443234.

E-mail address: scamarcio@fisica.uniba.it (G. Scamarcio).

conductivity may lead to largely inaccurate results [5]. Our approach to address this relevant problem is based on an experimental method for the measurement of the local lattice temperature on the facet of QCLs. This has been exploited in several previous studies of different classes of mid-IR and THz QCLs [6–11].

In this paper we present a study of the local lattice temperature distributions both from the laser facet and top surface of THz QCLs. The present results validate our approach and allow us to measure the lattice temperatures, the k_{\perp} values and the thermal boundary resistances (TBR). We have found that the TBR is the main physical parameter controlling heat transport in QCLs. In Section 3 we will discuss the role of interfaces on the thermal management of both mid-infrared and terahertz devices. Finally, in Section 4 we will report the observation of hot phonons in THz QCLs.

2. Experimental method

To extract the local lattice temperatures we performed microprobe band-to-band photoluminescence (PL) experiments. The PL signal was obtained by focusing the 647-nm line of a Kr^+ laser, working in continuous wave (CW) mode, either on the QCL front facet or on suitable apertures etched on the top surface of the device, down to a spot of about $1\ \mu\text{m}$ by using an $80\times$ long-working-distance plano-achromatic microscope objective lens. The Rayleigh scattering of the Kr^+ laser light has been blocked by means of a Notch filter. The devices were mounted into a helium-flow micro-cryostat and kept at a fixed heat sink temperature controlled with a calibrated Si-diode mounted close to the device. The sample position was varied by means of a piezoelectric translation stage with $0.1\text{-}\mu\text{m}$ spatial resolution. The signal was dispersed using a 0.64 m monochromator equipped with a single $110\times 110\text{ mm}^2$ grating with 600 lines/mm and detected with a Si charge coupled device (CCD) cooled to 140 K so that the dark current level is extremely low (less than 1 electron/pixel/hour).

The above method is based on the notion that the lattice temperature on the facet is a close estimate of the internal one. This assumption is related with the absence of non-radiative surface electron–hole recombination processes in unipolar devices. On the other hand, the latter is known to favor the formation of hot spots in conventional laser

diodes. Experimental investigations based on an interferometric bi-dimensional thermal mapping technique [12] showed that the temperature remains approximately constant along QCL waveguides.

Here we give further confirmation of this important point by measuring the longitudinal lattice temperature distribution in distributed feedback THz QCLs. We used surface emitting THz QCLs that offers the possibility of directly access the active region via a series of periodically spaced apertures located on the top surface along the waveguide [13].

The investigated device (sample c) is $45\ \mu\text{m}$ wide and 1.14 mm long and fabricated with 30 grating apertures $6\ \mu\text{m}$ wide on the surface. A schematic draft is shown in Fig. 1.

PL spectra have been recorded focusing the Kr laser in the middle of each aperture. The local lattice temperature (T_L) has been extracted by comparing the shift of the main PL peak against a calibration curve obtained by probing the device with zero injected current while varying the heat

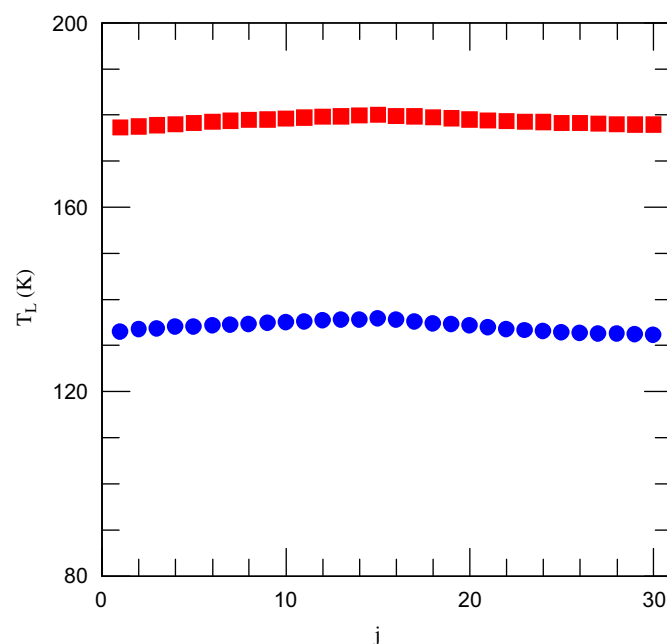


Fig. 2. Lattice temperatures (T_L) measured at a heat sink temperature $T_H = 75\text{ K}$ along the longitudinal axis of a surface emitting THz QCL, plotted as a function of the hole position (j), labeled as in Fig. 1, at $P = 2.1\text{ W}$ (■) and $P = 4\text{ W}$ (●).

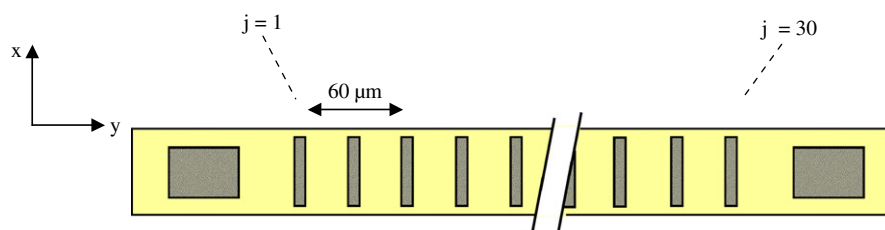


Fig. 1. Schematic of the top view of the grating structure of surface emitting QCLs.

sink temperature. The T_L values measured in $J = 1\text{--}30$ equally spaced grating apertures (see Fig. 1) are plotted in Fig. 2 as a function of hole position.

Our results demonstrate that T_L is approximately constant and less than $\sim 3\text{K}$ higher in the center of the axis with respect of the two sides. In all cases the T_L values increase linearly with P , with slopes $R_L = dT_L/dP$ coincident with the device thermal resistance. A value $R_L = 27.8 \pm 0.2\text{ K/W}$ has been extracted from the analysis of the PL spectra extracted from the different holes.

3. Thermal conductivity and Kapitza conductance

The cross-plane thermal conductivity k_{\perp} has been recently extracted by us in several classes of mid-IR QCLs by comparing experimental results on lattice temperature distributions with the outcome of theoretical calculations based on a 2D thermal modeling [14]. In THz QCLs the k_{\perp} values can be extracted directly from the experimental data, taking advantage from the absence of lateral heat extraction channels typical of mid-IR devices. Since the heat is uniformly distributed across the active region, the following relation holds:

$$T_L(z) = T_0 + \frac{P}{k_{\perp}S}z - k_2z^2,$$

where T_L is the lattice temperature measured in the active region, T_0 is the temperature at the interface between active region and lower cladding, P the power dissipated in the device, S the device area and k_2 a constant quantity.

Fig. 3 shows the experimental facet temperature profiles measured on two THz QCLs at a heat sink temperature $T_H = 45\text{ K}$. Device details are reported in Refs. [15,16], respectively.

We extracted the values $k_{\perp} = 5.4 \pm 0.5\text{ W/(K} \times \text{m)}$ and $k_{\perp} = 5.1 \pm 0.1\text{ W/(K} \times \text{m)}$ from the data of Figs. 3a and b, respectively. These values are ~ 1 order of magnitude lower than the relevant bulk ones at comparable temperatures. This can be explained considering the role of interfaces in the device thermal management. In fact, the parameter k_{\perp} can be expressed as a function of the bulk resistivities of the materials (R_i) and the average TBR that keeps into account the mean contribution of the interface resistivities. The following relation holds:

$$(k_{\perp})^{-1} = R_{\text{bulk}} - R_{\text{IF}} = \left(\sum_i (d_i/d_{\text{tot}})R_i + (N/d_{\text{tot}})\text{TBR} \right),$$

where d_i is the thickness of the GaAs, or AlGaAs layers in the active region, d_{tot} the total active region thickness and N the total number of interfaces.

In QCLs the bulk resistivity values have a negligible effect on the thermal conductivity of active regions. In fact, the latter is mostly determined by the high density of interfaces and hence by the second term in the above expression for $(k_{\perp})^{-1}$. The data of Figs. 3a and b allow to extract interface resistivity values $R_{\text{IF}} = 0.179\text{ K} \times \text{m/W}$ and $0.190\text{ K} \times \text{m/W}$, that accounts for 97% of the total device resistivity. Also we extracted $\text{TBR} = 1.28 \times 10^{-9}$ and $\text{TBR} = 1.35 \times 10^{-9}\text{ K/W m}^2$, respectively.

For a more extensive comparison we have compared in Table 1 the TBR values and the relative weight of the interface resistivity, measured in a set of mid-IR QCLs based on GaAs/AlGaAs [7], and GaInAs/AlGaAsSb [8] material systems. Our findings demonstrate that the thermal properties of QCLs are primarily controlled by heat transport phenomena taking place at the sharp heterostructure interfaces on a spatial extension of a few

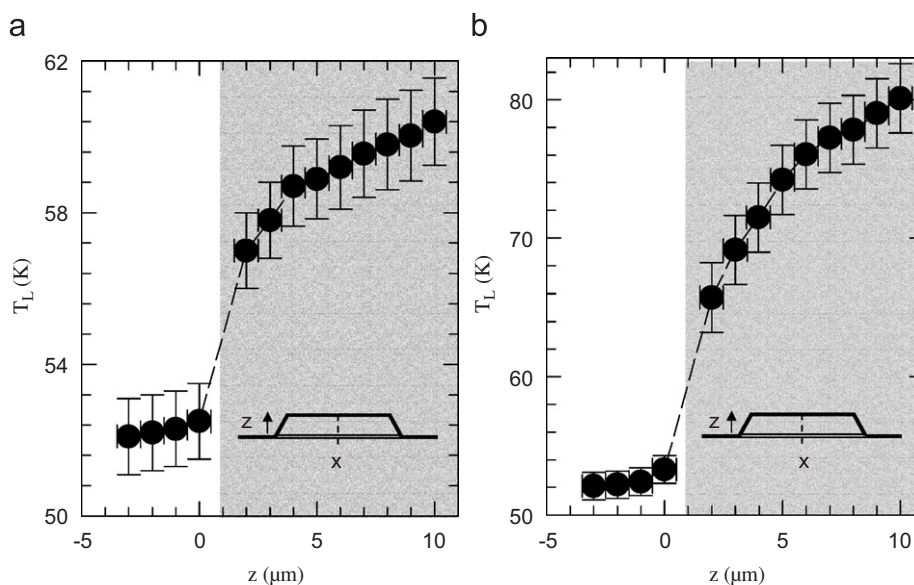


Fig. 3. Experimental temperature profiles measured along the growth axis in the center of the front facets of two QCLs operating at 2.9 THz (a) and 2.83 THz (b), driven by a CW electrical power of 1.1 W (a) and 3.8 W (b) at $T_H = 45\text{ K}$. The device dimensions are $250\ \mu\text{m} \times 1\text{ mm}$ (a) and $150\ \mu\text{m} \times 1\text{ mm}$ (b), respectively. The shaded area marks the active region layers.

Table 1

Cross-plane thermal conductivity, thermal boundary resistance and relative weight of the interface resistivity in a set of quantum cascade lasers, classified on the basis of the emitted wavelength and material system

Device material	λ (μm)	k_{\perp} (W/(K \times m))	TBR (10^{-9} K/(W \times m $^{-2}$))	IF resistivity
InGaAs/AlGaAsSb	4.9	2.0	0.58	49%
GaAs/Al _{0.33} Ga _{0.67} As	9.4	5.5	0.51	98%
GaAs/Al _{0.15} Ga _{0.85} As	105	5.4	1.28	97%
GaAs/Al _{0.15} Ga _{0.85} As	106	8.1	1.35	97%

monolayers, i.e. of the order of 1 nm. Future developments include the study of the influence of interface structure on the TBR and the exploitation of this knowledge for the development of new design strategies for the fabrication of QCL active regions having larger thermal conductivities.

4. Generation of non-equilibrium interface and longitudinal optical phonons

In bulk semiconductors, quantum wells and superlattices the electron–phonon interaction and the resultant phonon emission is the dominant process that controls the energy relaxation of carriers. The typical value for the e–LO (longitudinal optical) phonon scattering rate is $\sim(2\text{ps})^{-1}$ and the lifetime of optical phonons is in the range 3–9 ps. Thus if the excited carrier densities are sufficiently high, optical phonon emission can be so fast to raise the occupation number N of the strongly interacting modes above the thermal equilibrium value N_0 . This means that a non-equilibrium hot phonon population $N' = N - N_0$ can be generated. In GaAs quantum wells, the creation of non-equilibrium phonons does not only reduce the electron energy relaxation rate, but may also enhance the momentum relaxation rate. The latter effect arises if a complete randomization of the momentum of non-equilibrium phonons takes place during their lifetime. The presence of a hot phonon population strongly affects all main electronic transport and optical characteristics and leads to the enhancement of the phonon absorption rates, thereby reducing the net energy and momentum loss rates of carriers [17]. The hot-phonon effect has been accepted as the main factor responsible for the reduced cooling rate of hot carriers with a sheet density as high as 10^{10}cm^{-2} – 10^{12}cm^{-2} , as in the case of THz QCLs, which is also supported by theoretical results [17].

Energy relaxation of electrons, tunnel injected into excited subbands of QCLs, proceeds via intra- and inter-subband transitions, the dominant non-radiative channel generally being scattering by interface (IF) optical phonons. However, when energetically permitted, as in the case of resonant-phonon THz QCL, scattering due to electron–LO phonon interaction may have a significant role in inter-subband energy relaxation.

In a semiconductor multi-layered heterostructures the IF phonons are preferentially observed in backscattering from sample edge and it is possible to observe optical phonons related to the deformation potential only in the case of orthogonal polarizations between incident and scattered photons. This implies that IF phonons, transverse optical (TO) phonons and LO odd numbered confined phonons can be influenced by the deformation potential. Whereas, it is possible to observe optical phonons connected with the Fröhlich interaction only when the polarizations of incident and diffuse photons are parallel. Only even numbered confined LO and TO phonons and IF phonons are so influenced by this effect.

The devices investigated in the present work are resonant-phonon QC lasers that exploit the electron–phonon interaction to achieve population inversion between different conduction subbands.

In order to ascertain the existence of hot phonons in QCL structures, we have used a combination of microprobe Raman and PL measurements [18]. Raman experiments have been performed in backscattering configuration by using an edge emitting [12] or surface emitting [13] resonant-phonon THz QCL, respectively, in order to have access to both IF–TO or LO phonons. In backscattering condition the wavevector $q = 2k_y = 4\pi n(\lambda)/\lambda$. In our experiments the values $q = 0.75 \times 10^6\text{cm}^{-1}$, and $q = 1.1 \times 10^6\text{cm}^{-1}$ were used when the Kr⁺ laser wavelength was $\lambda = 647.1$ or 476.2nm , respectively. The employed power density was $P = 3 \times 10^4\text{Wcm}^{-2}$. The excitation wavelength has been chosen to avoid any resonant effect on the Raman spectra. At $\omega_L = 1.92\text{eV}$ only TO or transverse interface modes are not affected by electronic resonances, while to detect non-resonant LO phonons a frequency $\omega_L = 2.60\text{eV}$ should be used.

The observed Raman Stokes (S)/anti-Stokes (AS) spectrum yields an estimate of the phonon population. In fact, the ratio of the S/AS intensities for a given phonon mode, is related with the phonon population via the relation

$$\frac{I_S}{I_{AS}} = \frac{\sigma_S}{\sigma_{AS}} \frac{N+1}{N} \left(\frac{\omega_L - \omega_s}{\omega_L + \omega_s} \right)^4, \quad (1)$$

where N is the phonon occupation number and $\sigma_S(\omega_L)$ and $\sigma_{AS}(\omega_L)$ are the S and AS Raman cross sections at the laser frequency ω_L . A ratio $\sigma_{AS}/\sigma_S = 1.04 \pm 0.015$ has been extracted in both cases from the measurement of the ratio of the AS/S intensities as a function of the heat sink temperature, by probing the device with zero current.

The assessment of a non-equilibrium phonon population requires a comparison between the N values extracted from Raman scattering with the thermal equilibrium values N_0 . The latter information can be obtained using the microprobe PL technique exploited for the temperature mapping of THz QC lasers and described in the previous sections. The local lattice temperature of the device during operation

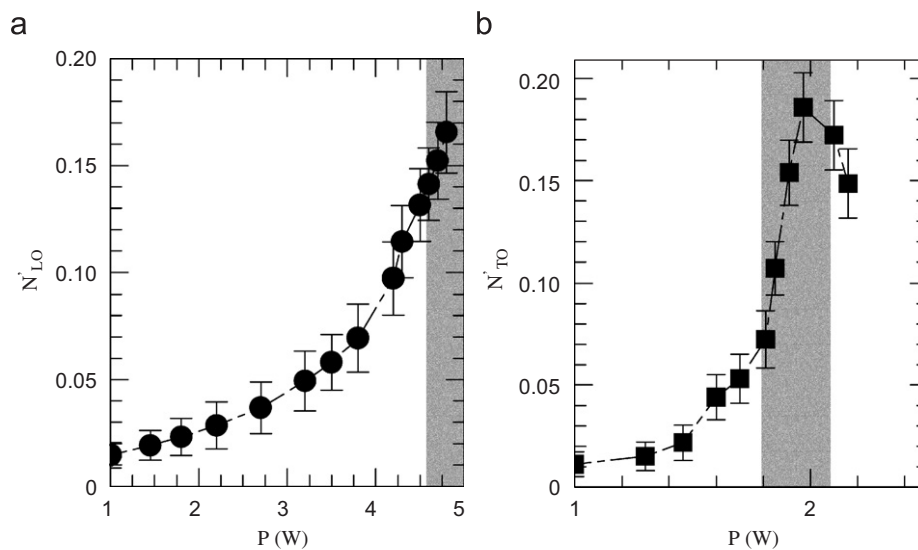


Fig. 4. Longitudinal optic (a) and transverse interface (b) GaAs non-equilibrium phonon occupation numbers as a function of the dissipated electrical power, measured at heat sink temperatures of 70 and 80 K, respectively. The shaded areas show the lasing region.

was obtained from the peak energy values of PL signals emitted by the active region layers.

Starting from the effective lattice temperatures T_L , extracted from PL measurements, we calculated the N_0 values from the following expression: $N_0 = 1/(1 - e^{h\omega/k_b T_L})$.

The N' values were calculated by means of Eq. (1). Excess interface and LO phonon occupation numbers has been found.

The dependence of the LO and IF hot phonon population on P are plotted in Figs. 4a and b for the surface emitting and edge emitting THz QCLs, respectively.

The superlinear increase of N' as a function of P in the lasing region can be tentatively ascribed to the occurrence of stimulated emission of phonons. The observation of linewidth narrowing of the anti-Stokes Raman bands would strengthen the above assignment. Preliminary results show no line narrowing. However, it should be considered that the stimulated emission of phonons is probably associated with electrons involved in laser transitions while the wall plug efficiency of the investigated THz QCLs is quite low (<1%). Moreover, since all the different GaAs wells composing the active region contributes to the Raman signal, the fluctuations of the GaAs layers width causes a phonon peak broadening which may hidden the observation of linewidth narrowing.

Acknowledgments

G.S., M.S.V. and V.S. acknowledge C. Sirtori and S. Barbieri for providing suitable QCL devices and for helpful discussions. Partial financial support from Regione Puglia, PE-056 is acknowledged.

References

- [1] G. Chen, Phys. Rev. B 57 (1998) 14958.
- [2] D.G. Cahill, W.K. Ford, K.E. Goodson, G.D. Mahan, A. Majumdar, H.J. Maris, R. Merlin, S.R. Phillpot, J. Appl. Phys. 93 (2003) 793.
- [3] W.S. Capinski, H.J. Maris, T. Ruf, M. Cardona, K. Ploog, D.S. Katzer, Phys. Rev. B 59 (1999) 8105.
- [4] S. Tamura, Y. Tanaka, H.J. Maris, Phys. Rev. B 60 (1999) 2627.
- [5] C. Gmachl, et al., IEEE Photonics Technol. Lett. 11 (1999) 1369.
- [6] V. Spagnolo, M. Troccoli, G. Scamarcio, C. Gmachl, F. Capasso, A. Tredicucci, A.M. Sergent, A.L. Hutchinson, D.L. Sivco, A.Y. Cho, Appl. Phys. Lett. 78 (2001) 2095.
- [7] V. Spagnolo, G. Scamarcio, D. Marano, M. Troccoli, F. Capasso, C. Gmachl, A.M. Sergent, A.L. Hutchinson, D.L. Sivco, A.Y. Cho, H. Page, C. Becker, C. Sirtori, IEEE Proc. Optoelectronics 150 (2003) 298.
- [8] M.S. Vitiello, G. Scamarcio, V. Spagnolo, A. Lops, Q. Yang, C. Manz, W. Bronner, K. Köhler, J. Wagner Appl. Phys. Lett. 90 (2007) 121109.
- [9] M.S. Vitiello, G. Scamarcio, V. Spagnolo, J. Alton, S. Barbieri, C. Worrall, H.E. Beere, D.A. Ritchie, C. Sirtori, Appl. Phys. Lett. 89 (2006) 021111.
- [10] M.S. Vitiello, G. Scamarcio, V. Spagnolo, B.S. Williams, S. Kumar, Q. Hu, J.L. Reno, Appl. Phys. Lett. 86 (2007) 111115.
- [11] M.S. Vitiello, G. Scamarcio, V. Spagnolo, L. Mahler, T. Losco, A. Tredicucci, H.E. Beere, D.A. Ritchie, Appl. Phys. Lett. 88 (2006) 241109.
- [12] C. Pflugl, M. Litzemberger, W. Schrenk, D. Pogany, E. Gornik, G. Strasser, Appl. Phys. Lett. 82 (2003) 1664.
- [13] S. Kumar, B.S. Williams, Q. Qin, A.W.M. Lee, Q. Hu, Opt. Express 15 (2006) 113.
- [14] A. Lops, V. Spagnolo, G. Scamarcio, J. Appl. Phys. 100 (2006) 043109.
- [15] S. Barbieri, J. Alton, H.E. Beere, J. Fowler, E.H. Linfield, D.A. Ritchie, Appl. Phys. Lett. 85 (2004) 1674.
- [16] M.S. Vitiello, G. Scamarcio, V. Spagnolo, S.S. Dhillon, C. Sirtori, Appl. Phys. Lett. 90 (2007) 191115.
- [17] P. Lugli, S.M. Goodnick, Phys. Rev. Lett. 59 (1987) 716.
- [18] V. Spagnolo, G. Scamarcio, M. Troccoli, F. Capasso, C. Gmachl, A.M. Sergent, A.L. Hutchinson, D.L. Sivco, A.Y. Cho, Appl. Phys. Lett. 80 (2002) 4303.